

# Compton scattering, the electron mass, and relativity: A laboratory experiment

P. L. Jolivet and N. Rouze  
Hope College, Holland, Michigan 49423

(Received 21 May 1993; accepted 18 October 1993)

Compton scattering in a semiconductor detector is used to “discover” the relativistic relation between energy and momentum and to demonstrate the dependence of  $p$ ,  $E$  and  $\gamma$  on  $\beta$ . The motivation is to measure the (rest) mass of the electron, and this can be done to within 1 keV with a commonly available set of gamma ray sources. To determine precisely where the Compton edge occurs in a spectrum, a Monte Carlo calculation of detector response is described which also helps the student to understand the physics of the detection process.

## I. INTRODUCTION

In modern physics courses Compton scattering is introduced to emphasize the particle nature of photons and the recoiling electron is largely ignored. However, with commonly available gamma ray sources the kinetic energy of the recoiling electron is often on the order of 1 MeV and the electrons are indeed relativistic. Compton scattering is a convenient source of relativistic particles in the undergraduate laboratory, and when it occurs in a detector the kinetic energy of the recoiling electron is directly measured. In this report we describe how such measurements can be used to determine the relativistic relations between energy, momentum, and mass for the recoiling electron simply and precisely. The experiment is initially presented to the students as a measurement of the electron mass to complement an  $e/m$  experiment and the Millikan oil drop determination of the charge of the electron. The student's analysis is forced onto an instructive detour due to the obvious inadequacy of the nonrelativistic equations. The process leads to the discovery, based on the data, of the energy-momentum relation of special relativity.

Experiments to measure the mass of the electron<sup>1</sup> and the relativistic relations for the electron<sup>2</sup> using the Compton edge have been published previously, but these reports did not emphasize the discovery approach or the precision possible. Measurements of the Compton angular distribution with the intent of discovering the form of the relativistic relations have also been described,<sup>3</sup> but this is a more complicated experiment and requires a high intensity source of gamma rays.

## II. THE ANALYSIS

The experiment consists of measuring the energy of the Compton edge from ordinary gamma ray spectra as a function of the energy  $E_\gamma$  of the incident gamma rays. The Compton edge corresponds to the kinetic energy  $T$  of the recoiling electron when the incident gamma ray is scattered through  $180^\circ$ . To achieve the best results, the Compton edge energy must be measured with high precision, and we recommend the use of a germanium detector. Further, to avoid systematic errors it is important to understand the shape of the spectrum, and models to describe the shape are discussed in Sec. III.

The data used in this report are listed in Table I and Fig. 1 shows a plot of  $T$  vs  $E_\gamma$ . The best that can be said about these variables is that they are indeed the measured quantities. The relation between them, whether derived classically or relativistically, provides little insight to the student. The fact that the dependent and independent parameters are not simply related is the greatest barrier to using this experiment with unsophisticated students.

There are only four ideas needed to analyze the data; the realization that the gamma ray is a photon, conservation of energy and momentum in the collision, and the classical relation  $E_\gamma = p_\gamma c$  between the energy and momentum of an electromagnetic wave or photon. For the Compton edge, the energy of the electron corresponds to an incident photon scattered through  $180^\circ$  and conservation of momentum gives

$$p_\gamma = p - p'_\gamma, \quad (1)$$

where  $p_\gamma$ ,  $p'_\gamma$ , and  $p$  are the momenta of the incident gamma ray, the scattered gamma ray, and the recoiling electron, respectively. Conservation of energy gives

$$p_\gamma c = p'_\gamma c + T. \quad (2)$$

These relations may be combined to give the electron momentum in terms of the experimental variables,

$$pc = 2E_\gamma - T. \quad (3)$$

The above does not rely in any way on special relativity.

As a first attempt to determine the electron mass, we can assume the nonrelativistic relation,  $T = p^2/2m_{nr}$ , so that the (rest) energy of the electron is given in terms of the experimental quantities by

$$m_{nr}c^2 = \frac{p^2c^2}{2T} = \frac{(2E_\gamma - T)^2}{2T}. \quad (4)$$

When the calculated values of  $m_{nr}c^2$  are plotted as a function of  $T$ , Fig. 2, it is immediately obvious that  $m_{nr}c^2$  is not constant. But the surprising result is that, to within experimental uncertainties, the dependence on  $T$  is linear with a slope of  $1/2$ . Furthermore, the intercept is equal to the value of  $m_0c^2$  which the student should expect from the low energy  $e/m$  and Millikan experiments, or from the “book value.” Replacing the left-hand side of Eq. (4) with this experimental result,  $m_0c^2 + T/2$ , gives

$$p^2c^2 = 2Tm_0c^2 + T^2. \quad (5)$$

The addition of  $(m_0c^2)^2$  to complete the square gives

$$p^2c^2 + (m_0c^2)^2 = (T + m_0c^2)^2 = E^2, \quad (6)$$

where  $E$  is the total energy of the electron. This is the central energy-momentum relationship of special relativity.

Table I. Measured Compton edge energies.

Source	$E_\gamma$ (keV)	$E_{\text{Compton}}$ (keV)
$^{60}\text{Co}$	1173.2	$963.5 \pm 1.0$
$^{60}\text{Co}$	1332.5	$1117.0 \pm 1.0$
$^{137}\text{Cs}$	661.7	$477.0 \pm 1.0$
$^{22}\text{Na}$	511.0	$339.0 \pm 1.0$
$^{22}\text{Na}$	1274.5	$1061.0 \pm 1.0$
$^{133}\text{Ba}$	356.0	$207.0 \pm 1.0$
$^{207}\text{Bi}$	569.7	$393.0 \pm 1.0$
$^{207}\text{Bi}$	1063.7	$858.0 \pm 1.0$
$^{207}\text{Bi}$	1770.2	$1547.0 \pm 1.0$
$^{152}\text{Eu}$	344.3	$196.0 \pm 1.0$
$^{152}\text{Eu}$	1408.0	$1190.0 \pm 1.0$
$^{208}\text{Tl}$	2614.5	$2382.0 \pm 2.0$
$^{116}\text{In}$	416.9	$263.0 \pm 2.0$
$^{116}\text{In}$	1097.3	$890.0 \pm 2.0$
$^{116}\text{In}$	1293.0	$1079.0 \pm 2.0$
$^{116}\text{In}$	2112.1	$1883.0 \pm 2.0$
$^{57}\text{Co}$	122.1	$39.0 \pm 1.0$
$^{241}\text{Am}^a$	59.5	$11.3 \pm 0.5$
$^{57}\text{Co}^a$	122.1	$39.3 \pm 0.5$

<sup>a</sup>Measured with a Si(Li) detector.

Once Eq. (6) has been “discovered” it can be solved to calculate directly the rest energy as originally asked of the student. This procedure differs from using the intercept of Fig. 2 since relativity is now assumed to be the correct theory. In terms of the measured quantities,

$$m_0c^2 = \frac{p^2c^2 - T^2}{2T} = \frac{2E_\gamma(E_\gamma - T)}{T} \quad (7)$$

The calculated values of  $m_0c^2$  are plotted as a function of  $T$  in Fig. 3, and the mass is clearly seen to be independent of the kinetic energy. Statistical errors of about  $\pm 1$  keV in  $m_0c^2$  are possible, but systematic errors of about the same magnitude are also present largely due to residual errors in actually locating the Compton edge, see Sec. III below.

The student has now reached the stated goal of measuring the (rest) mass of the electron. In addition the data can be manipulated to verify other common relativistic rela-

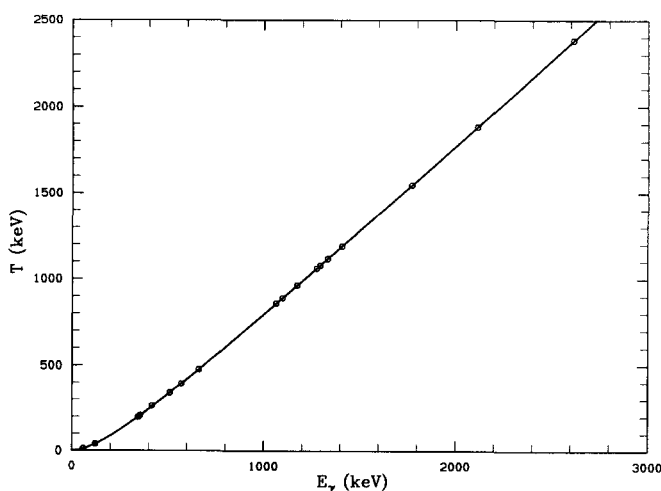


Fig. 1. The electron kinetic energy as a function of  $E_\gamma$ . The line is a fit of  $T = 2E_\gamma^2 / (2E_\gamma + m_0c^2)$  [from Eq. (7)] which yields  $m_0c^2 = 512.7 \pm 0.9$  keV. The uncertainties are smaller than the data points.

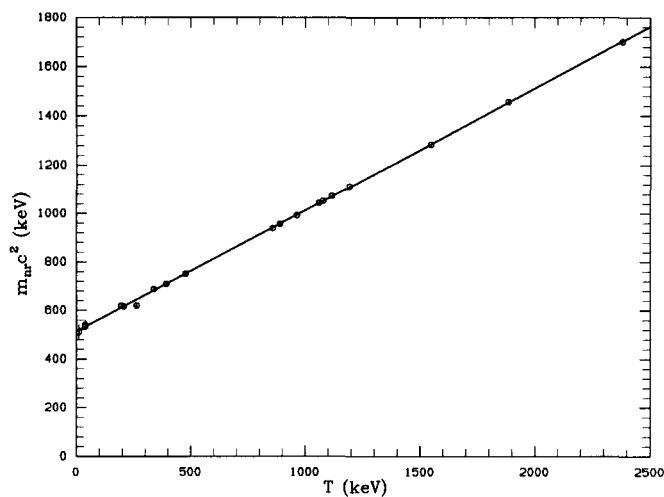


Fig. 2. The electron rest energy calculated nonrelativistically and then fitted with a linear relationship. There are uncertainties in both directions which are usually smaller than the points. The intercept is  $513.6 \pm 1.9$  keV and the slope is  $0.4991 \pm 0.0016$ .

tions. To determine the electron velocity, or equivalently  $\beta = v/c$ , we use the relativistic mass  $m$  and the relations  $p = mv$  and  $E = mc^2$  to give

$$\beta = \frac{v}{c} = \frac{m_0c}{m} = \frac{pc}{E} = \frac{2E_\gamma - T}{T + m_0c^2} = \frac{T(2E_\gamma - T)}{T^2 - 2E_\gamma T + 2E_\gamma^2} \quad (8)$$

Figure 4 shows the plot of  $pc$  vs  $\beta$ . For the 2.615 MeV gamma ray from  $^{208}\text{Tl}$ ,  $\beta = 0.984$ , and the plot clearly shows the expected asymptotic behavior as  $\beta$  approaches unity.

A plot of  $E$  vs  $\beta$  also shows the expected asymptotic behavior. The total energy  $E$  is expressed in terms of the experimental measurements as

$$E = T + m_0c^2 = \frac{T^2 - 2TE_\gamma + 2E_\gamma^2}{T} \quad (9)$$

The relativistic factor  $\gamma$  can be calculated from the relation  $E = \gamma m_0c^2$  so that

$$\gamma = \frac{E}{m_0c^2} = \frac{m_0c^2 + T}{m_0c^2} = 1 + \frac{T^2}{2E_\gamma(E_\gamma - T)} \quad (10)$$

Figure 5 plots  $\gamma$  vs  $\beta$ . For reasons discussed below  $\gamma$  is calculated from the relation  $\gamma = E/m_0c^2$  using the value of  $m_0c^2$  determined in Fig. 3 rather than the last form of Eq.

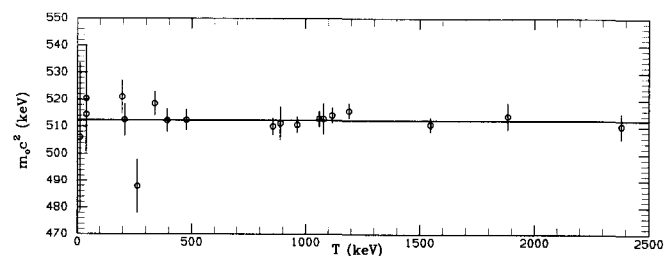


Fig. 3. The electron rest energy vs electron kinetic energy when calculated relativistically. There are uncertainties in both directions. The uncertainties in  $m_0c^2$  are large at low energies since  $d(m_0c^2)/dT$  is large there. For this data set  $m_0c^2 = 512.7 \pm 0.9$  keV identical to that in Fig. 1.

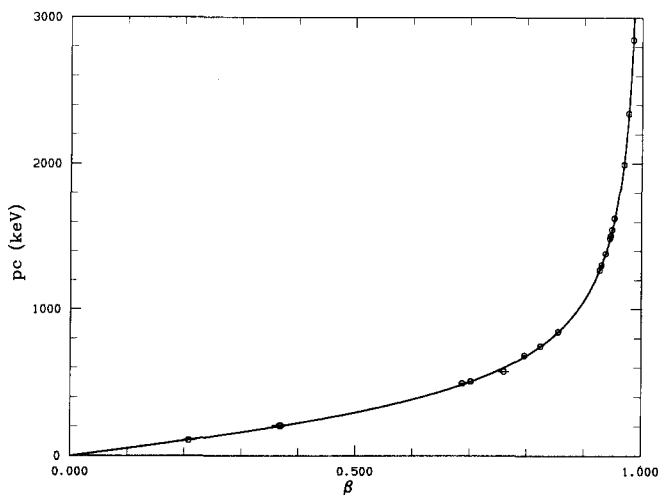


Fig. 4. Electron momentum as a function of  $\beta$ . There are errors on both axes which are usually smaller than the points. The line is  $pc = \gamma\beta m_0 c^2$ .

(10). The expected relation  $\gamma = 1/(1 - \beta^2)^{1/2}$  is seen to hold.

The analysis described above emphasizes the discovery of the energy-momentum relation and confirms the velocity dependence of  $pc$ ,  $E$ , and  $\gamma$ . Consequently, all plotted variables are expressed in terms of the measured quantity  $T$  and the independent variable  $E_\gamma$ . Error bars should be calculated, displayed and used in the fitting process even though they are very often smaller than the data points as plotted. In a precision experiment that both determines an important quantity,  $m_0$ , and elucidates an important theory, the fact that you cannot see the error on the paper does not mean that it is unimportant in defining the certitude with which one accepts the result.

Note that in many of the plots there are errors on both the ordinate and the abscissa. Most students have not been introduced to techniques to handle such data properly. While the difficulty can be ignored in the process of dis-

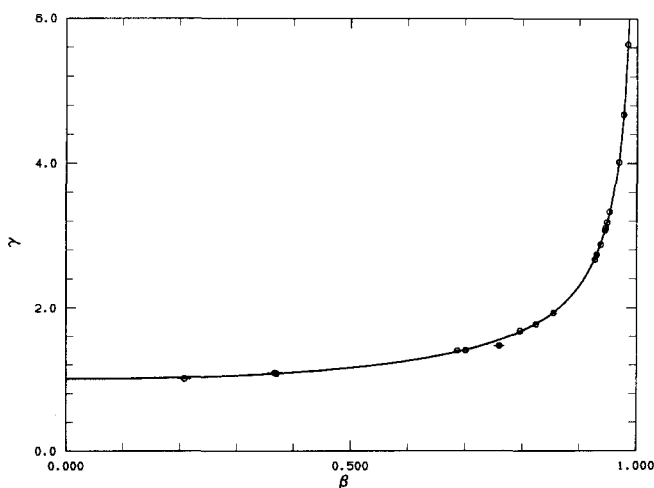


Fig. 5. A plot of  $\gamma$  vs  $\beta$  where  $\gamma = E/512.7$  [i.e., not calculated with the last form of Eq. (10)]. There are uncertainties in both directions which are usually smaller than the points. The line is a fit with  $\gamma = 1/(a + b\beta^2)^{1/2}$  which yields  $a = 0.989 \pm 0.008$  and  $b = -0.988 \pm 0.009$ .

covering the need for a relativistic treatment, errors in both coordinates can be treated easily when determining the uncertainty in the results.<sup>4</sup>

The last remarks might be considered a bit disingenuous as there are several subtleties hidden in the analysis above. The first is that the uncertainty in the rest mass found from the fit in Fig. 2 is larger than the uncertainties calculated in the fits of Fig. 1 or Fig. 3. The latter two give identical errors even though one is a nonlinear fit and the other is a simple average. The reason is that one is fitting two parameters in the case of Fig. 2 and only one in the other cases. The extra parameter, the slope of Fig. 2, defines the energy-momentum equation of special relativity, Eq. (6). The other two fits assume that relativity is the correct theory, and so all the statistical precision in the measurements appears in the fitted value of the mass.

The second point is that in the cases where there are errors in both plotted coordinates the uncertainties are always correlated and are not independent. This arises because there is only one measured variable  $T$  for each datum and the uncertainty in each coordinate is determined from the uncertainty in the measured value of  $T$ . The plotted variables are not measured separately and independently. The normal procedures for fitting data assume that the uncertainties are independent, i.e., random. The procedures characterized by Figs. 1 and 3 are free of this defect. The first because one is really fitting the dependent and independent variables and the second because the averaging process ignores the value of the abscissa and its error. For the cases of  $m_{nr}c^2$  vs  $T$ ,  $pc$ , and  $E$  vs  $\beta$  the correlations are not serious. But for  $\gamma$  vs  $\beta$  the correlation is perfect if the last form of Eq. (10) is used to calculate  $\gamma$ , rather than dividing  $E$  by the average value of  $m_0c^2$ . In other words, any two randomly chosen numbers with  $E_\gamma$  greater than  $T$  and relations (8) and (10) give values of  $\beta$  and  $\gamma$  which are related by  $\gamma = 1/(1 - \beta^2)^{1/2}$  since this relation is implicit in Eq. (6).

### III. DETECTOR CHARACTERISTICS

The experiment can be carried out with a NaI(Tl) detector, but the much better energy resolution of a semiconductor, HPGc, Ge(Li), or Si(Li), detector allows one to make very precise measurements and to use sources with fairly complex spectra. However, the excellent resolution of the full energy peak in a semiconductor detector does not translate directly into as great an improvement in the sharpness of the Compton edge. There are two primary reasons. First, for monoenergetic gamma rays there is a background in the region of the Compton edge even for a "perfect" detector, and second, the electron struck in the collision is bound and, consequently, is not at rest. For a monoenergetic gamma ray the most important source of background is events where there are multiple Compton scatterings in the detector, but not all the gamma ray energy is lost. All backgrounds should be subtracted before the edge is determined, but it is still necessary to have a method to find the location of the edge since it is not perfectly sharp in the experimental spectrum and one would like precision on the order of 1 keV.

A simple argument shows that the Compton edge should exhibit a vertical drop in the gamma ray yield at the appropriate energy. The Compton edge corresponds to gamma rays scattered at  $180^\circ$  since we have two particle elastic scattering and, kinematically, this angle corre-

sponds to the maximum energy for the recoiling electron. Experiments<sup>5</sup> measuring the scattered gamma ray show that the cross section does not go to zero at this angle. Thus there should be a finite number of electrons scattered into each channel of the spectrum up to the maximum allowed energy and then the drop to zero.

Experimentally the edge is not sharp but falls from a near plateau to the multiple scattering background with a rounded edge shape, almost like the right half of a Gaussian distribution. Combining these ideas gives a model of a cross section with a sharp drop at the edge energy convoluted with a Gaussian smearing function. From a typical <sup>137</sup>Cs spectrum the Gaussian can be estimated to have  $\sigma \sim 5$  keV. This width is significantly greater than the width of the full energy peak, so there is clearly other physics involved than simply the noise in the system.

A model consisting of a constant scattering cross section below the edge convoluted with a Gaussian indicates that the true edge is located halfway down the drop. This model is quite robust; the smearing need not be Gaussian but only symmetric with a characteristic width much less than the edge energy to get a result very near 0.5. If the underlying spectrum is not flat (and the Compton spectrum is not) there is again only a small correction.

To determine better where the Compton edge is located in an actual spectrum a Monte Carlo simulation was done to unravel the various features. The details of the detector response result from intrinsically interesting physics and can promote a better appreciation in the student that a good understanding of the instrumentation is necessary for precision measurements. Writing a Monte Carlo simulation is a reasonable student project, but not of the one-week variety.

A good introduction to the behavior of gamma ray detectors is found in Knoll.<sup>6</sup> However, the region of the Compton edge is not usually of prime importance in their use, except in so far as the background can be suppressed. The Monte Carlo simulation allows one to find which mechanisms produce the various features of the spectrum including the details near the edge.

The primary energy loss mechanisms for gamma rays are the photoelectric effect, Compton scattering and pair production. Compton scattering is dominant in the region of interest from a few hundred keV to a few MeV. However, Compton scattering does not annihilate the gamma ray but only shifts it to lower energy where it can interact again. Most gamma rays which end up in the full energy peak undergo more than one Compton scattering followed by a photoelectric interaction. The gamma rays which undergo multiple Compton scatterings but escape the detector before the photoelectric interaction contribute to the background which extends into the region between the Compton edge and the full energy peak. They create the prominent bulge which is seen at energies above the Compton edge. This and all other backgrounds must be taken into consideration in locating the edge.

The shape of the spectrum due to single Compton scattering events in a "perfect" detector followed by immediate escape of the energy shifted gamma ray is given by the Klein-Nishina formula<sup>6</sup> which predicts a rise in the yield as the high energy limit is approached followed by a discontinuous drop to zero which defines the edge. This dependence gives the broad peak seen in spectra just below the Compton edge. In a real detector the edge is never

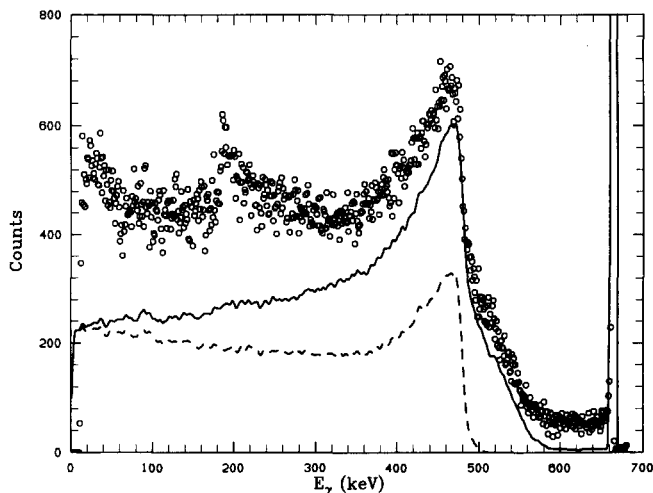


Fig. 6. Monte Carlo calculation for the 0.662 MeV gamma ray of <sup>137</sup>Cs (—). The dashed line (---) is the calculation for the single Compton scattering events. The open circles are the experimental spectrum with room background subtracted. The calculation is normalized to give the same number of counts in the photopeak as the experimental spectrum and has been smoothed.

perfectly sharp but is convoluted with a resolution function. If the width of this smearing were the full energy peak resolution, about 2 keV, it would not be serious, but the major contributor is the Fermi motion of the struck electron which is bound to the germanium atom. As the K electron binding energy is about 11 keV, the spreading is considerable.

Figure 6 compares the measured spectrum to the Monte Carlo result for the 0.662 MeV gamma ray of <sup>137</sup>Cs in our 9% HPGe detector of closed end coaxial design along with the spectrum due to single Compton interactions. The logic of the simulation program generally follows that of Meixner.<sup>7</sup> The elements of the process were (1) monoenergetic gamma rays enter through the detector dead layers where a few interact and are shifted in energy; (2) the path length to the interaction point in the detector is selected randomly based on exponential attenuation proportional to the total cross section; (3) if the gamma ray has not escaped the detector, in which case the tracking terminates and the energy deposited recorded, the type of interaction is selected randomly according to the relative cross sections for the three interaction modes; (4) the recoil energy of the struck electron is assumed to be fully absorbed by the detector. The calculation for this photon terminates if this is a photoelectric event; (5) the new path of a Compton scattered gamma ray is chosen randomly according to the Klein-Nishina angular distribution and the new energy calculated for that angle. For a pair production event two 0.511 MeV gamma rays are created going in opposite directions. The residual gamma rays from both mechanisms are tracked by going back to step (2) and the summed energy lost in all interactions is eventually saved.

There are a number of simplifications assumed in the above process. Some electrons escape the detector, but a rather simple model indicated that this loss made little difference to the result since the electron ranges are usually small compared to the size of the detector. There is a dead region in the core of the crystal which was ignored as was

the effect of imperfect charge collection. Escaping bremsstrahlung and characteristic x rays were also ignored.

The most important additional effect controlling the shape of the Compton edge is the Fermi motion of the struck electron.<sup>8</sup> This was treated in an approximate fashion as a full treatment would be complicated by the alteration of the Klein–Nishina angular distribution due to the electron’s motion which should be treated with relativistic kinematics. Instead the scattering angle is chosen randomly from the distribution defined by the Klein–Nishina formula and the photon and electron energies calculated. Then the energies were modified by randomly selecting a momentum transfer in the collision with a probability weighted according to the distribution for the germanium electron momentum transfer.<sup>9</sup> The data from Ref. 9 were parametrized as the sum of three Gaussians each representing a different electron shell and weighted by the number of electrons in the shell. [A variant of the program using the appropriate parameters for a Si(Li) detector was also used.]

In Fig. 6 the area of the photopeak is normalized to the data. (The dimensions of the detector crystal had been adjusted to match the measured photopeak efficiency for the 1.333 MeV gamma ray from <sup>60</sup>Co.) The simulation is gratifyingly best near the Compton edge and is of similar quality in comparison to other sources with different gamma ray energies. The shape of the Compton edge is satisfactory although the amplitude is about 10% too low. This fault is probably related to the deficit in the number of counts at the minimum between the Compton edge and the photopeak.

The Monte Carlo results were used to develop an algorithm to locate the true position of the Compton edge which is reliable in the presence of backgrounds, moderate statistics, and the spreading of the edge. Any method based on finding the position of the maximum in the Compton distribution fails because the peak is broad and flat and cannot be located with sufficient accuracy to be useful. A simple and stable process is to find the maximum height of the peak and then the height of the background at the foot of the Compton edge which is created by multiple Compton scatterings and other processes, i.e., where the “bulge” meets the edge. (The Monte Carlo calculation indicates that the most tightly bound K electrons create a foot on the single Compton distribution which is not experimentally distinguishable from the other background components, Fig. 6.) The energy of the Compton edge corresponds to the energy where the data rises to a point midway between these two values, see Fig. 7. This criterion is the same as suggested by the descriptive argument above. The exact correspondence arises from the approximations made after the Monte Carlo calculation to make the process stable with reasonable statistics.

The scatter in the Monte Carlo results is believed to come from statistical fluctuations and the result of binning the data. For simulations with an incident gamma ray energy of less than about 1.5 MeV and 1 keV bins, the channel corresponding to the average height is always within  $\pm 1$  keV of the true value. The edge is found in the spectrum where the yield is changing most rapidly so that fluctuations and individual biases in selecting the various points seldom cause a deviation of more than one channel in the chosen edge position. The biggest sources of systematic uncertainty are the precision of the Monte Carlo cal-

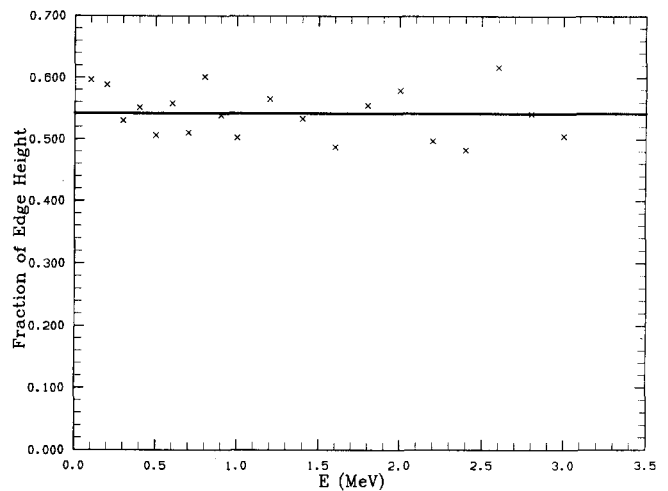


Fig. 7. The position of the Compton edge determined from the Monte Carlo simulation is located at a fraction  $f$  of the height of the rise due to the single Compton scattering events. If  $y_t$  is the yield at the top of the Compton peak,  $y_c$  is the yield at the position of the Compton edge and  $y_b$  is the yield in the background at the base of the peak then  $f = (y_c - y_b) / (y_t - y_b)$ . The average fraction is  $f = 0.54$  with a standard deviation of 0.04.

ulation and the subjectivity in selecting the yield at the base of the Compton edge which arises from the foot caused by the tightly bound electrons. A student who tends to include this foot in the background will have a bias to too low an energy for the edge while one who puts the base at the point where the foot just comes in will be too high. The Monte Carlo program is available on request.<sup>10</sup>

#### IV. EXPERIMENTAL CONSIDERATIONS

With a germanium detector most of the common gamma ray sources will give a satisfactory spectrum to identify the Compton edge. A set consisting of <sup>60</sup>Co, <sup>22</sup>Na, and <sup>137</sup>Cs is just sufficient to measure the rest energy to within approximately 1.5 keV. However, to demonstrate the relativistic relations a wider range of energies is recommended. The addition of <sup>133</sup>Ba and <sup>207</sup>Pb extends the range from 0.356 to 1.770 MeV. Alternatively, these can be replaced by <sup>152</sup>Eu as the lines at 0.344 and 1.408 MeV each give a useful Compton edge. These are all long lived isotopes and thus convenient. To extend the range even further the 2.615 MeV gamma ray from the thorium daughter <sup>208</sup>Tl is the highest energy usually available. If a source is not on hand the room background from an overnight run is often just sufficient or there might be a few hundred grams of a thorium salt in your chemistry store room. If a neutron source is available irradiation of indium gives a line at 2.112 MeV which augments the high energy range.

All of the above isotopes result in electrons with  $\beta > 0.6$ . Sources which give clean Compton edges at low energies are rare and usually short lived. The K x rays of heavy elements, e.g., <sup>207</sup>Pb, are too complex and have too much background to provide good data, but the 122 keV line from <sup>57</sup>Co works well. There is some extra uncertainty due to extrapolating the calibration to such a low energy. The 53 keV line from <sup>133</sup>Ba is visible in our detector, but the 35 keV x rays are not. The Compton edge is clear at 39 keV (a

fact for the student to ponder as gamma rays of this energy are almost completely attenuated) so the extrapolation is not too great.

The low energy range is easily measured with a Si(Li) detector. Since it is possible to use x rays for calibration, the extrapolation problem does not exist. An extremely low energy datum is available using a  $^{241}\text{Am}$  source with this detector. One of the Np L x rays falls on the edge, but a thin absorber, e.g., 0.3 mm of Cu, suppresses the x rays without attenuating the 59 keV gamma ray significantly and gives a clean Compton edge at 11 keV. Note that these two low energy points do little to constrain the value of  $m_0c^2$  since from Eq. (7) the error in the rest energy is magnified for low  $T$ , i.e.,  $d(m_0c^2)/dT$  approaches infinity as  $T$  approaches zero. Consequently, a measurement of the Compton edge for  $^{241}\text{Am}$  with an uncertainty of 0.1 keV yields an uncertainty greater than 5 keV in  $m_0c^2$  and the effect is seen in Fig. 3. These low energy data do make the plots where  $\beta$  is the abscissa much more convincing.

The error in the measurement of the Compton edge is about  $\pm 1$  keV if the dispersion of the spectra is about 1 keV per channel and there are at least 300 counts per channel. It should be remembered that Compton scattering will be more important in a small detector than a large one which will have a higher probability of multiple scatterings. This means, however, that there is a low efficiency for high energy gamma rays. Most spectra can be taken in 5 to 15 min with source intensities of 1 to 10  $\mu\text{Ci}$  although the high energy points often take longer.

## V. CONCLUDING REMARK

The experiment described above is easy to carry out and analyze and provides a convincing experimental demonstration of the necessity of special relativity and a precise

measurement of the electron rest mass. The theory only requires a modern physics course. The difficulty that so many of the interesting, and often displayed, relations, e.g.,  $p$  vs  $\beta$ , are flawed by the effects of correlated uncertainties should be pointed out to the student. We end our discussion with the suggestion that the student describe an experiment which does not suffer from this problem. The usual, and satisfactory, answer is to measure the velocity and momentum of a particle separately. For example, a velocity selector followed by the measurement of the radius of curvature in a magnetic field. Such an experiment is simpler in concept but more difficult in execution than the present experiment.

<sup>1</sup>T. S. Mudhole and N. Umakantha, "Determination of the rest-mass of the electron: A laboratory experiment," *Am. J. Phys.* **45**, 1119–1120 (1977).

<sup>2</sup>J. Higbie, "Undergraduate relativity experiment," *Am. J. Phys.* **42**, 642–644 (1974).

<sup>3</sup>Matthiam J. H. Hoffman, "The Compton effect as an experimental approach toward relativistic mass," *Am. J. Phys.* **57**, 822–825 (1989).

<sup>4</sup>P. L. Jolivet, "Least-squares fits when there are errors in  $X$ ," *Comput. Phys.* **7**, 208–212 (1993).

<sup>5</sup>R. P. Singhal and A. J. Burns, "Verification of Compton collision and Klein–Nishina formulas—An undergraduate laboratory experiment," *Am. J. Phys.* **46**, 646–649 (1978).

<sup>6</sup>G. F. Knoll, *Radiation Detection and Measurement*, 2nd ed. (Wiley, New York, 1989).

<sup>7</sup>Ch. Meixner, "A Monte Carlo program for the calculation of gamma-ray spectra for germanium detectors," *Nucl. Instrum. Methods* **119**, 521–526 (1974).

<sup>8</sup>J. Felsteiner, S. Kahane, and B. Rosner, "Effect of the electron-momentum distribution on the shape of the Compton edge of Si(Li) detectors," *Nucl. Instrum. Methods* **118**, 253–255 (1974).

<sup>9</sup>W. A. Reed and P. Eisenberger, "Gamma-ray Compton profiles of diamond, silicon and germanium," *Phys. Rev. B* **6**, 4596–4604 (1972).

<sup>10</sup>The program is available on request. Requests for direct transfer can be made to "jolivet@physics.hope.edu" on Internet.

## Dispersion-free linear chains

Matthias Reinsch

*Department of Physics, University of California at Berkeley, Berkeley, California 94720*

(Received 19 April 1993; accepted 13 September 1993)

General formulas are given for the masses and spring constants of one-dimensional finite chains with linear dispersion relations, examples of which were given by Herrmann and Schmälzle in 1981 in their discussion of a well-known collision apparatus. The mathematical similarity to the problem of a Boson in a constant magnetic field is shown. The explicit formulas make a study of the continuum limit possible. This is shown to be related to the system of uniform rods studied by Bayman in 1976. Examples are given of chains with quadratic dispersion relations. Resonances that give singularities in the interaction time are discovered in certain chains of elastic spheres.

## I. INTRODUCTION

Numerous papers<sup>1</sup> have been written on the ball collision apparatus shown in Fig. 1. When playing with such a device, people usually get the impression that if  $n_{\text{in}}$  balls are drawn aside and released,  $n_{\text{in}}$  balls will move away at the

far end after the collision, the remaining balls being motionless (this occurrence will be called "perfect transmission" in this paper). There is also an impressive list<sup>2</sup> of books in which it is claimed that for the case of elastic balls, this outcome is determined by the laws of conserva-